Half-metallic character and electronic properties of inverse magnetoresistant $Fe_{1-x}Co_xSi$ alloys

Javier Guevara,[1,2,*] Verónica Vildosola,[2,3] Julián Milano,[2,3] and Ana María Llois[2,3]
[1]*Escuela de Ciencia y Tecnología, Universidad de San Martín, Alem 3901, (1651) San Martín, Argentina*
[2]*Departamento de Física, CAC-CNEA, Avenida Gral. Paz 1499, (1650) San Martín, Argentina*
[3]*Departamento de Física, FCEN-UBA, Pab. I, Ciudad Universitaria, (1429) Buenos Aires, Argentina*
(Received 17 October 2003; revised manuscript received 10 March 2004; published 28 May 2004)

Based on *ab initio* calculations we find that $Fe_{1-x}Co_xSi$ alloys in the Fe-rich region behave as a disordered ferromagnetic half metal. Half metallicity can explain the recently found electronic, magnetic, and transport properties. We can also determine a sharp transition from the paramagnetic metallic behavior to the ferromagnetic half-metallic state as a function of Co concentration. At concentrations higher than 0.25 the system starts to segregate Co from Fe atoms, this giving rise to the disappearance of half metallicity and to reflect it in the decreasing value of the magnetic moment.

DOI: 10.1103/PhysRevB.69.184422 PACS number(s): 75.50.−y, 71.23.−k, 75.90.+w

I. INTRODUCTION

The discovery of giant magnetoresistance in 1988 (Ref. 1) triggered a new era in the modeling of materials for which the spin degree of freedom is the relevant variable. The main challenge in spintronics[2] (spin-based electronics) is to build devices that can be used as sources of strong spin-polarized currents (spin currents). In the search for these devices half metals are thought to be good candidates as highly spin-polarized electron sources.

Half metallicity is an unusual combination of metallic and insulating properties in a single system in which one spin channel is metallic and the other semiconducting. This type of magnetic material was discovered by de Groot[3] in 1983. The semiconducting behavior of one of the channels leads to an integer magnetic moment per cell in stoichiometric compounds or proportional to doping electrons in doped systems. No spin-flip processes occur at low energies, which would give rise to a spin susceptibility that vanishes with applied magnetic field.[4] For a half-metallic magnet to exist the presence of narrow bands and gaps in the energy spectrum is necessary, as well as strong magnetic interactions.[4]

$Fe_{1-x}Co_xSi$ alloys have been extensively studied[5,6] and still go on revealing surprising properties. It has been recently shown that these disordered alloys present a remarkable behavior, particularly in the Fe-rich region: the magnetic moment depends linearly on Co concentration x suggesting a fully spin-polarized electron gas, the magnetization saturates at low applied magnetic fields H, and an inverse or positive magnetoresistance, that is, increasing resistance in response to an increasing H, is observed.[7] The relevant experimental feature of these systems is that the electrons responsible for the magnetic properties are those for the electric transport as well. It is the electron-electron quantum interference that gives rise to a new mechanism for magnetoresistance in ferromagnets.

Both parent compounds FeSi and CoSi, as well as their mixtures $Fe_{1-x}Co_xSi$, have a common crystal structure B20 (spatcial group $P2_13$), in which all transition-metal atoms are crystallographically equivalent. While both extrema are nonmagnetic, a ferromagnetic order appears at intermediate concentrations.

FeSi is a small gap semiconductor and there are still controversies on how to explain the anomalous behavior of some of its properties, especially the susceptibility and specific heat have an unusually strong temperature dependence.[8] Many different theoretical attempts have been tried to describe this system, such as spin fluctuations,[9] Fermi-liquid behavior,[10] or Kondo-like insulator.[11] However, band-structure calculations within the local-density approximation (LDA) agree well with low-temperature measurements.[12] On the other hand, CoSi is a diamagnetic metal which has been less studied.[5]

$Fe_{1-x}Co_xSi$ alloys are isostructural with the parent compounds along the whole concentration range. They do not form compounds and their lattice parameters are proportional to x.[13] Thereafter they seem to be systems in which the physical properties are mostly governed by the doping electrons.

We show in this work that the magnetic and transport properties observed in the Fe-rich region of $Fe_{1-x}Co_xSi$ are due to their half-metallic character.

II. APPROXIMATIONS USED AND METHODS OF CALCULATION

We study the electronic properties of the series $Fe_{1-x}Co_xSi$ within band theory, performing calculations with the WIEN code,[14] which is an implementation of the full potential linearized augmented plane-wave method within density functional theory. We use the exchange-correlation potential in the local-spin-density approximation.[15] The considered *muffin tin* ratios R_{mt} are 2.1 a.u for the transition-metal (TM) atoms and 2.0 a.u. for Si. The cutoff parameter which gives the number of plane waves in the interstitial region is taken as $R_{mt}K_{max}=9$, where K_{max} is the maximum value of the reciprocal-lattice vector used in the expansion of plane waves in that zone. The number of **k** points in the Brillouin zone is enough in each case to obtain the desired energy and charge convergence.

The systems under study show a very closed-packed structure. The unit cell is cubic, with lattice parameter a, and contains 4 f.u. (formula units). Each TM atom has seven Si nearest neighbors (one at $0.51a$, three at $0.52a$, and three at

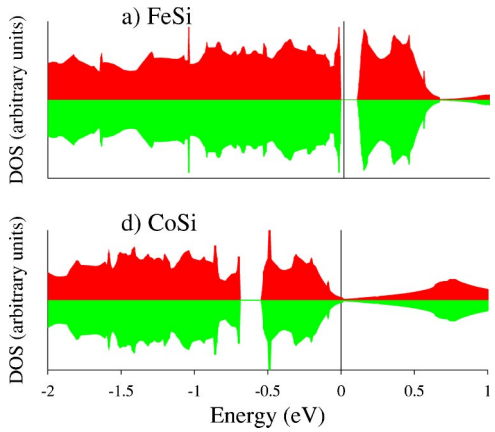

FIG. 1. Total density of states for (a) FeSi and (b) CoSi. Both DOS's are very similar, E_F lying in each case at very different positions, in a *d*-band gap for FeSi and in a depressed region for CoSi. The Fermi level is set equal to zero.

0.56a) and six TM next-nearest neighbors at 0.61a. For FeSi the obtained equilibrium lattice parameter is $a=4.37$ Å, while for CoSi $a=4.36$ Å.

Our results for FeSi agree well with previous calculations.[16,17] Both parent systems turn out to be nonmagnetic, FeSi resulting a semiconductor with a narrow band gap in the middle of the Fe *d* band and CoSi a (semi)metal, in agreement also with experiments. In Fig. 1 we show the densities of states (DOS's) for FeSi and CoSi. It can be clearly seen that both DOS's are very similar, the difference resulting just from a rigid shift of the Fermi level E_F when interchanging Fe by Co. In the Case of FeSi, E_F lies in a gap in the middle of the *d* band showing a high density of states near the band edges. On the contrary, E_F of CoSi lies in an energy region where the DOS is very low as it is the case of semimetals.

To study the doped system in the Fe-rich region we use two complementary approaches. The first approach makes use of the virtual crystal approximation[18,19] (VCA) and considers a single B20 unit cell in which each Fe atom has been assigned an extra noninteger charge to account for doping concentrations. Charge neutrality is preserved in the calculations. In this approximation it is assumed that doping electrons are homogeneously distributed among the TM atoms, all TM atoms are equivalent while the chemistry of the disordered alloys is not fully taken into account.

To check the VCA procedure and to obtain conclusive results we implement a second approach by doing supercell calculations (SCC) for different Co concentrations and for several configurations. For a given concentration x, we build different arrangements by substituting Fe atoms by Co ones within single, double, or triple B20 unit cells, containing from 4 to 12 f.u. per supercell.

We finally obtain, at a given concentration x, a weighted average magnetic moment from different arrangements by using a Boltzmann distribution. For this calculation we take into account the energies of each configuration and the experimental annealing temperature as the Boltzmann factor.

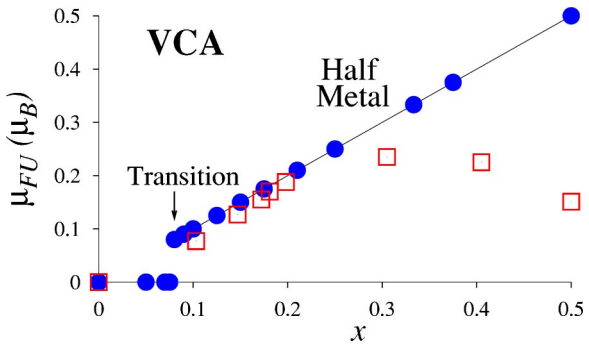

FIG. 2. Calculated magnetic moment per f.u. within VCA. We show the metal–half-metal transition at $x=0.08$ and half-metallic character since then up to $x=0.5$. □ are the experimental results of Ref. 7.

III. RESULTS

A. Virtual crystal approximation

The VCA is usually taken as a reasonable approximation for a small amount of doping electrons. In spite of this, we have extended it to values of x going from 0 to 1. In particular for $x=1$, the obtained DOS is similar to the one shown above for CoSi (Fig. 1). The system is half metallic up to 0.5, at this concentration the majority band becomes semimetallic. For values of x larger than 0.5 the minority band starts to populate and the system becomes metallic with a magnetic moment which decreases with x. This procedure helps us to obtain some insight into the evolution of the system with x and has been successfully applied in the whole concentration range to $Fe_{1-x}Co_xSi_2$.[19]

In Fig. 2 we show the VCA results for the magnetic moment per f.u. as a function of x up to 0.5. Half-metallic character appears at $x=0.08$ and remains up to 0.5. The system behaves as a nonmagnetic metal for low doping concentrations and has then a sharp transition to a half-metallic character. These results have encouraged us to check the half-metallic character of these systems using a better approach, and also to find out why this character persists up to high concentrations within the VCA approximation, while experimentally the magnetic moment decreases beyond $x=0.25$.

In Fig. 3 we show the DOS obtained within VCA for $x=0.2$; the half-metallic character is clearly observed. The fact that the injected charge only populates the majority band is a result of the balance between kinetic and exchange energies. This balance and the presence of the gap in the energy

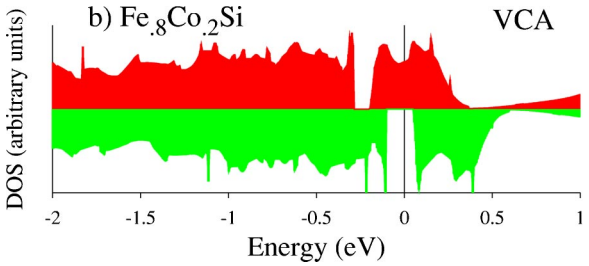

FIG. 3. DOS of $Fe_{0.8}Co_{0.2}Si$ within VCA. It can be clearly seen that the Fermi level lies in a gap of the minority band and in the middle of the Fe *d* states of the majority band.

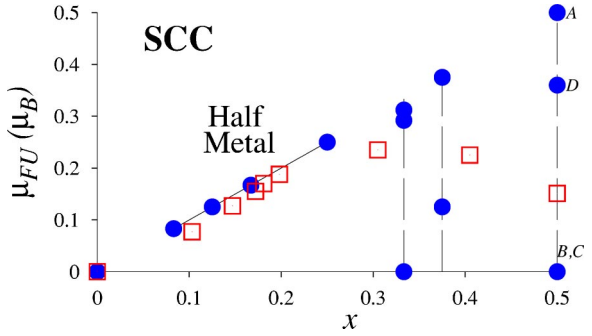

FIG. 4. Calculated magnetic moment per f.u. within the SCC approach. A half-metallic character is found in almost the whole concentration region, but only between $x=0.083$ and 0.25 is the half-metallic one, the only solution for all the arrangements tried. For $x=0.1667$ the three different arrangements considered show half-metallic character. For $x=0.5$ (a), (b), (c), and (d) correspond to calculations done for the different structures shown in Fig. 6. □ are the experimental results of Ref. 7.

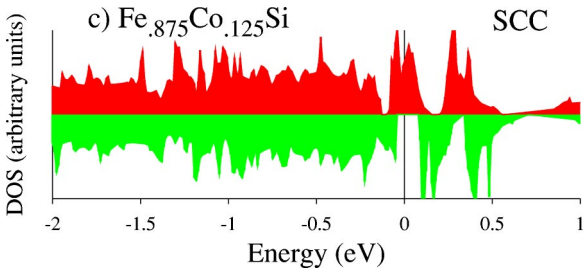

FIG. 5. DOS of the half-metallic $Fe_{0.875}Co_{0.125}Si$ alloy calculated with the SCC approach, it can be clearly seen that the majority (up) band is metallic while the minority (down) is semiconducting. Fermi level is equal to zero.

spectrum explain the preference of the doping charge to become fully spin polarized, as discussed in Ref. 19. At very low doping, exchange is not large enough to overcome the kinetic energy, and the system behaves as a nonmagnetic metal. By using VCA, an approximation which allows for a continuous doping, we obtain the abrupt transition from a nonmagnetic metal to a ferromagnetic half metal. This energy competition is then present in this approach.

B. Supercell calculations

Within the SCC approximation the influence of the chemical and local environment is taken into account. For each concentration a weighted average over the different atomic configurations should be performed in order to obtain DOS and magnetizations. The systems studied within SCC are those with $x=0.083$, 0.125, 0.167, 0.250, 0.333, 0.375, and 0.500, built by using single, double, and triple supercells. For $x=0.083$ and 0.125 only one arrangement can be performed to keep the cell size tractable. We consider two configurations for $x=0.250$, three for $x=0.167$, 0.333, and 0.375, and four different configurations for $x=0.500$. These different arrangements at a fixed concentration allow us to survey the effects of the local environment on the determination of the magnetic order of the systems.

In the very low-concentration region we calculate for only one atomic arrangement ($x=0.083$), for which the Co atoms do not show any kind of CoSi segregation. Configurations showing CoSi segregation would demand larger supercells to keep the same concentration.

1. Low concentration region (**0.083≤x≤0.25**)

For concentrations ranging from 0.08 to 0.25, VCA and SCC give the same results: we obtain a linear dependence of the magnetic moment per f.u. ($\mu_{f.u.}$) on x, in agreement with experiments. The linear behavior is obtained independently of the considered atomic arrangement. See Figs. 2 and 4.

In Fig. 5 we show the DOS obtained within SCC for $x=0.125$. It is clearly observed that the majority (up) band is metallic while a gap appears at the Fermi level for the minority (down) band. With both approximations, VCA and SCC, a half-metallic character is obtained even if the SCC DOS shows more structure than the VCA one.

It is important to point out that not only the Co atoms are magnetic but that the total magnetic moment is distributed among Co and Fe atoms, although some Fe atoms (those which are not Co nearest neighbors) have a negligible local magnetic moment. The Fe magnetic moment varies from $0.1\mu_B$ to $0.5\mu_B$, depending on x and on the chosen supercell. For instance, in the case of $x=0.167$ the three configurations here considered show a half-metallic character while the Co local environment changes from one configuration to the other.

In order to get insight and to quantify the influence of the local environment on the appearance of half metallicity, we define $NN_{Co}(TM)$ as the number of Co atoms which are nearest neighbors of a given TM atom. For $x=0.167$ three configurations are considered. In the first configuration $NN_{Co}(Co)$ is zero (for the two Co atoms within the supercell). The second configuration has a value of $NN_{Co}(Co)$ equal to 1, while in the third configuration it rises to 2, this being the last configuration, the one with the lowest total energy. For $x=0.083$ and 0.125, $NN_{Co}(Co)=1$.

In the case $x=0.25$ one of the selected arrangements shows a value of $NN_{Co}(Co)=0$ while in the other one $NN_{Co}(Co)=2$, being this last arrangement, the lowest-energy one. For this concentration, the arrangement with the largest $NN_{Co}(Co)$ has the lowest energy as well.

For those concentrations for which more than one arrangement has been considered, the configurations showing the largest segregation [largest $NN_{Co}(Co)$] are the minimum-energy ones even if keeping their half-metallic character in this concentration range.

2. High-concentration region (**0.25<x≤0.50**)

For values of x larger than 0.25 the experimental magnetic moment decreases monotonously to zero with increasing x. Here the results of both approaches split as can be seen comparing Figs. 2 and 4. Within VCA the magnetic moment per f.u. continues growing linearly with x. The experimental evolution of μ can be understood by analyzing the SCC results for different configurations at a given value of x, each of them providing partial information about the real system.

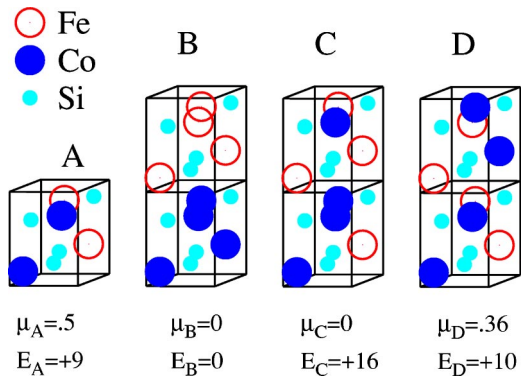

FIG. 6. Four configurations with $x=0.5$. Structure (a) corresponds to the single B20 cell where all Co's (all Fe's) are equivalent. In structure (b) Fe's and Co's are completely segregated. Structures (c) and (d) represent different intermixed configurations. Open spheres correspond to Fe atoms, solid spheres to Co atoms, and the small ones to Si atoms. We give the resulting magnetic moment per f.u., μ, in units of μ_B, and the relative total energies E in millirydbergs.

In this concentration range we have done SCC calculations for $x=0.333$, 0.375, and 0.500. In the particular case of $x=0.5$ we consider the four different configurations shown in Fig. 6. The single B20 cell, structure (a) in Fig. 6, represents the most homogeneous distribution at this concentration and μ_B is very close to $0.5\mu_B$. For this configuration in which Co's and Fe's are homogeneously distributed within the cell, the magnetic moment follows the linear dependence on x (as it happens within the VCA approximation). But for those configurations in which there exist CoSi regions completely separated from FeSi ones [full segregation, structure (b)], the magnetic moment is zero. For the other particular configurations having the same concentration, structures (c) and (d), in which Fe's and Co's are intermixed, the calculated magnetic moments per f.u. are $\mu_{f.u.}=0.0\mu_B$ and $0.36\mu_B$, respectively.

If we focus on the total energies of these configurations, structure (a) has the highest relative energy while structure (b) has the lowest. The experimental saturated magnetic moment at $x=0.5$ is less than $0.2\mu_B$, which should be considered as a weighted average over the magnetic moments of all possible configurations at this concentration. In Fig. 6 we also give the relative total energies with respect to the one obtained for structure (b), which presents a $\mu_{f.u.}=0.0\mu_B$ and where Fe's and Co's are completely segregated. The values of NN_{Co}(Co) for each of the inequivalent Co atoms are 2 in the case of structure (a), and 3 and 5 for structure (b). For structure (c), which has four inequivalent Co atoms, we have NN_{Co}(Co) equal to 1, 2, 2, and 3, and finally for structure (d) the obtained values for NN_{Co}(Co) are 1 and 3.

For $x=0.333$ we perform calculations for three different supercell configurations (not shown). None of them is a half metal, although two arrangements present a high $\mu_{f.u.}$. The first one presents $\mu_{f.u.}=3.51\mu_B$ and $NN_{Co}(Co)=0$, the second one shows $\mu_{f.u.}=3.74\mu_B$ and $NN_{Co}(Co)=2$, while the third configuration has $\mu=0$ and values of NN_{Co}(Co) equal to 3 and 5 for the inequivalent Co's. The last one also shows the lowest energy among the three configurations.

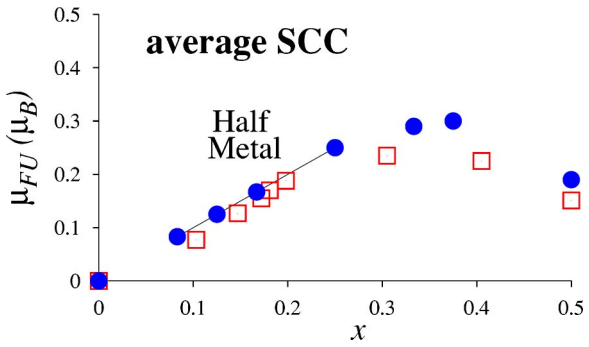

FIG. 7. Weighted average magnetic moments per f.u. within the SCC approach. It can be seen that these magnetic moments (*circle*) follow closely the experimental curve. □ are the experimental results of Ref. 7.

For $x=0.375$ we do calculations for three configurations as well. For two of them $\mu_{f.u.}=x\mu_B$ while for the third one $\mu_{f.u.}=0.124\mu_B$. The first configuration presents NN_{Co}(Co) values equal to 1 and 2 for the inequivalent Co's. The second arrangement presents NN_{Co}(Co) values equal to 0 and 2, and the third one 3 and 4. The last arrangement is the lowest total-energy one.

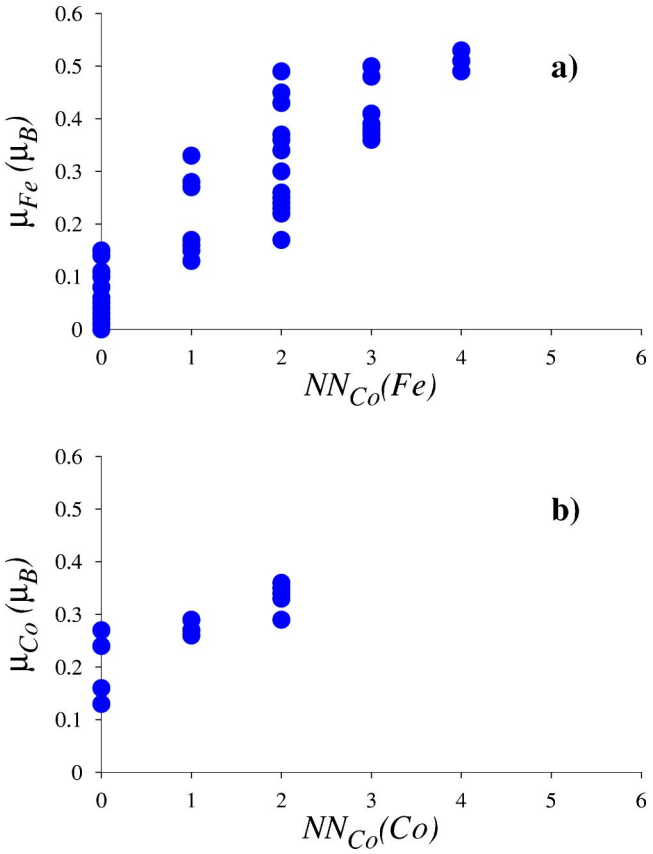

FIG. 8. Local magnetic moments of the TM atoms, corresponding to all the calculated arrangements that present half-metallic character, vs NN_{Co}(TM). (a) corresponds to Fe atoms and (b) to Co atoms. In (a) we can see that μ_{Fe} increases with NN_{Co}(Fe) while (b) shows that the non-half-metallic solution appears for NN_{Co}(Co) larger than or equal to 3.

3. Weighted average magnetic moments

By taking into account the energy differences among all the considered arrangements at a given concentration x within the SCC approximation, we have estimated the magnetic moment per f.u. making a weighted average over all these configurations. We have used a Boltzmann distribution to calculate the relative weight of each configuration at the experimental annealing temperature.[7] In Fig. 7 we show the values obtained for $\mu_{f.u.}$ by this procedure. The curve follows closely the experimental trends.

C. Local environment

From the examples treated above we obtain an overview of the dependence of the properties of the $Fe_{1-x}Co_xSi$ system on local environment. In Figs. 8(a) and 8(b) we show the evolution of the local magnetic moment of the different Fe and Co atoms as a function of NN_{Co}(TM) for all the concentrations and arrangements studied, which show half-metallic character. It is seen that, if the half-metallic character is present, the magnetic moment of both Fe and Co atoms increases with NN_{Co}(TM). The Fe-Co hybridizations enhance the magnetic moment of the TM atoms when the system is half metallic.

From Fig. 8(b) we see that if NN_{Co}(Co) is larger than or equal to 3 the system is not half metallic. In other words Fe-Co hybridization triggers a magnetic ordering in these systems and the larger the value of NN_{Co}(Fe) the bigger the magnetic moment. However if NN_{Co}(Co) goes beyond a limiting value, the system loses its half-metallic behavior. We have then two competing effects with increasing Co concentration, namely, Fe-Co hybridization which enhances $\mu_{f.u.}$ and CoSi aggregation which tends to destroy the magnetic order and thereafter the half metallicity.

IV. DISCUSSION AND CONCLUSIONS

Half metallicity of $Fe_{1-x}Co_xSi$ alloys for $x=0.25$ explains the experimentally observed fast saturation of the magnetization with an applied magnetic field, giving rise to a vanishing magnetic susceptibility typical of half-metallic magnets. What makes out of this system an interesting one is that many of the known half metals have crystalline order and lose the half-metallic character with little disorder. This is not the case for $Fe_{1-x}Co_xSi$ for which disorder and half metallicity go together. However half metallicity in these systems is not as robust as in $Fe_{1-x}Co_xS_2$,[19] where half metallicity takes place from $x=0.25$ to 0.9.

Through comparison with experiments and our total-energy *ab initio* calculations we suggest that in the Fe-rich region the samples are neither completely segregated nor completely intermixed and that half metallicity disappears beyond $x=0.25$. The system loses the linear dependence of the magnetic moment on x when the segregation of FeSi from CoSi grows in importance. This is the reason for the observed decrease of the magnetic moment, which is closely related to the disappearance of half metallicity. We infer that the transition from the half-metallic state to a ferromagnetic metal is not sharp and that it probably depends on sample preparation conditions.

With respect to the magnetoresistant behavior of these systems observed in Ref. 7, Manyala *et al.* claim that transport electrons are the same that give rise to magnetization. They arrive to this conclusion because their magnetotransport results can be explained within the theory of diffusive transport in disordered systems,[20,21] where the quantum interference effects lead to an enhancement of the Coulomb interactions.[22] The half-metallic behavior that we find in these alloys gives ground for this scenario but a theoretical frame including half metallicity in disordered systems is still lacking.

In summary, we can satisfactorily explain the evolution of the magnetic moment of $Fe_{1-x}Co_xSi$ with x within band theory and a nearly one-electron picture. Actually LDA underestimates correlation effects, but it reproduces very well the magnetic behavior of these alloys in the Fe-rich region at very low temperature as we have shown. The most interesting conclusion we come to is that the linear dependence of the magnetic moment on x is due to the half-metallic character of these mixed systems, present for $0.08 \leqslant x \leqslant 0.25$. This fact increases even more its appeal for future technological applications in the realm of spintronics because they are disordered ferromagnetic half metals that can be grown without strain on the parent semiconducting FeSi. Beyond $x=0.25$ we conclude that segregation is getting more and more important and, consequently, the magnetic moment decreases monotonously towards zero with increasing x.

ACKNOWLEDGMENTS

We want to thank A. Fert and R. Weht for useful discussions. This work was partially supported by Contract No. UBACyT X115, Fundación Sauberan, Fundación Balseiro, and by Fundación Antorchas. A.M.L. and J.G. are researchers of CONICET.

*Electronic address: Javier.Guevara@unsam.edu.ar

[1] M.N. Baibich, J.M. Broto, A. Fert, F. Nguyen Van Dau, F. Petroff, P. Ettienne, G. Creuzet, A. Friederich, and J. Chazalas, Phys. Rev. Lett. **61**, 2472 (1988)

[2] S.A. Wolf, D.D. Awschalom, R.A. Buhrman, J.M. Daughton, S. von Molnár, M.L. Roukes, A.Y. Chtchelkanova, and D.M. Treger, Science **294**, 1488 (2001).

[3] R.A. de Groot, F.M. Mueller, P.G. van Engen, and K.H.J. Buschow, Phys. Rev. Lett. **50**, 2024 (1983).

[4] W.E. Pickett and J.S. Moodera, Phys. Today **54** (5), 39 (2001).

[5] J.H. Wernick, G.K. Wertheim, and R.C. Sherwood, Mater. Res. Bull. **7**, 1431 (1972).

[6] S. Kawarazaky, H. Yasuoka, Y. Nakamura, and J.H. Wernick, J. Phys. Soc. Jpn. **41**, 1171 (1976).

[7] N. Manyala, Y. Sidis, J.F. DiTusa, G. Aeppli, D.P. Young, and Z. Fisk, Nature (London) **404**, 581 (2000).

[8] V. Jaccarino, G.K. Wertheim, J.H. Wernick, L.R. Walker, and S. Arajs, Phys. Rev. **160**, 476 (1967).

[9] Y. Takahashi, J. Phys.: Condens. Matter **9**, 2593 (1997); **10**, L671 (1998).
[10] S. Misawa and A. Tate, J. Magn. Magn. Mater. **157**, 617 (1996).
[11] C. Fu, M.P.C.M. Krijin, and S. Doniach, Phys. Rev. B **49**, 2219 (1994).
[12] T. Jarlborg, Phys. Rev. B **59**, 15 002 (1999).
[13] D. Shinoda, Phys. Status Solidi A **11**, 129 (1972).
[14] P. Blaha, K. Schwarz, and J. Luitz, computer code WIEN97 (Vienna University of Technology, 1997) [Improved and updated Unix version of the original copyrighted WIEN code, which was published by P. Blaha, K. Schwarz, P. Sorantin, and S.B. Trickey, Comput. Phys. Commun. **59**, 399 (1990)].
[15] J.P. Perdew and Y. Wang, Phys. Rev. B **45**, 13 244 (1992).
[16] L.F. Matheiss and D.R. Hamann, Phys. Rev. B **47**, 13 114 (1993).
[17] E.G. Moroni, W. Wolf, J. Hafner, and R. Podloucky, Phys. Rev. B **59**, 12 860 (1999).
[18] N.J. Ramer and A.M. Rappe, Phys. Rev. B **62**, R743 (2000).
[19] I.I. Mazin, Appl. Phys. Lett. **77**, 3000 (2000).
[20] P.A. Lee and T.V. Ramakrishnan, Phys. Rev. B **26**, 4009 (1982).
[21] P.A. Lee and T.V. Ramakrishnan, Rev. Mod. Phys. **57**, 287 (1985).
[22] P. Chen, D.Y. Xing, and Y.W. Du, Phys. Rev. B **64**, 104402 (2002).